Journal of Heat and Mass Transfer Research

Semnan University

Investigation of particle resuspension from a garment using different turbulence dispersion models

Hamidreza Kharinezhad Arani, Ali Jafarian *, Jamal Darand

Faculty of Mechanical Engineering, Tarbiat Modares University, P.O. Box 14115-143, Tehran, Iran.

ABSTRACT

One of the most important sources of aerosol production in a controlled space is the human. The flow around the individual and the particles on the garment play an essential role in aerosol distribution in the environment. Such spaces are simulated from a Lagrangian or Eulerian point of view. In this research, particle resuspension from a user's garment under horizontal and vertical unidirectional systems was studied. For this purpose, a computer program was developed and used for examination of the impacts of different particle turbulence dispersion models, such as Discrete Random Walk, in a controlled space. Moreover, the effects of flow direction, velocity, and particle density on the probability of resuspension of particles with different diameters were investigated. The results demonstrated that the vertical *unidirectional* system had advantages over its horizontal variant, and that increased flow velocity provided positive feedback in the vertical system but negative feedback in the horizontal one. In the horizontal system, the resuspension probability for the sizes of 5 and 0.5 microns has increased by 177 and 355 percent, respectively, compared to the vertical system. It is worth noting that the results of the isotropic and non-isotropic models for particles size below 5 microns were quite the same. For the particles size over 5 microns, the maximum percentage discrepancy of 138 in resuspension probability between the non-isotropic and isotropic models is obtained.

1. Introduction

Interior air quality is a very important issue, which is of even greater significance in a controlled space such as a clean room, a space with controlled pollutant and aerosol levels much lower than in common interior spaces. The main purpose of designing a clean space is to control the amount of pollutant particles in the area. For categorization and specification of the application of a controlled space, the number of aerosols in the room volume is used as criterion. This demonstrates the significance of air quality and accuracy in the calculations made for these spaces. The number of aerosols that are there depends on different factors such as resuspension of particles from surfaces or particle-producing sources [1,2]. One of the most important sources of particles is the user of the controlled space, producing most of the aerosols. To simulate the space, an Eulerian or a Lagrangian approach needs to be adopted. In a Lagrangian approach, several models of particle turbulence dispersion are presented, each with its own accuracy, advantages, and disadvantages.

The literature involves two areas. One includes cases where particle turbulence dispersion models are used. Over the years, several studies have been carried out on the effects of different such models in particle deposition in channels and similar conditions. Some notable examples from the above area of research follow. Tian and Ahmadi [3] studied the effects of different boundary conditions beside the wall on particle deposition rate. The impacts of turbulence on particle dispersion and deposition were examined using Discrete Random Walk (DRW) and Continuous Filtered White-Noise (CFWN), and the accuracy and validity of simulation of the two turbulence models in

*Corresponding Author: Ali Jafarian
Email: jafarian@modares.ac.ir

the current field was discussed. They showed that the DRW and CFWN turbulent dispersion models are both capable methods for modeling particle velocity fluctuations in the turbulent flow of the channel. Gao et al. [4] also conducted a study of the effects of turbulent flow models on duct deposition results, and provided a correction factor for the DRW model. They found that the RSM model can successfully predict the transition from the diffusion region to the inertia-moderated region. Mito and Hanratty [5] used the Langevin equation to describe turbulent dispersion of fluid particles in a channel flow. The difference between these models in simulation of controlled environments has not yet been studied, as they have been used commonly to inspect deposition in very small ducts. Kang and et al. [6] studied the influence of temperature and vertical location of inlet supply air in a displacement ventilation room. In their study, discrete random walk (DRW) model was utilized to simulate the stochastic velocity fluctuations in the airflow. The results showed that the inlet location would slightly influence the ventilation efficiency.

Detachment and resuspension of particles is an important source of aerosol concentration in interior spaces [2]. Understanding air current and, subsequently, aerosol suspension due to human factors, such as movement, provides some insight on mechanisms of concentration variation in interior spaces. Research in this area includes studies on simulation of the human walk model and its effects on concentration. Due to the complexity of this movement, some researchers have considered it as a falling-disc or footstep motion [2, 7-9]. Kubota and et al [6] experimentally investigated the human foot movement and particle resuspension from the floor. Zhao, & Zhang [9] simulated the movement of foot walking. The movement of foot can cause the resuspension of ground particles. Indoor human activities can cause resuspension of particulate matter in space. Boulbair et al. [10] studied CFD (using DRW model) of the unsteady airflow field around and under the shoe. They showed that Particle resuspension fractions increased with particle size and walking speed. Sun et al. [11] performed a series of experiments to study the coupling effects between human walking and ventilation condition on indoor particle resuspension.

Qian, & Ferro [13] reviewed the particle resuspension due to human walking in indoor environments. They concluded that particles resuspension is an important source for indoor particulate matter compared to other indoor sources. In addition, they showed that resuspension increases with particle size in the range of 0.7-10 μm. Sajadi et al. [12] used Fluent and DRW to simulate resuspension of particles and examine the particle surface resuspension rate resulting from the fall of a disc. One of the most notable studies on resuspension of

particles in the room is the experimental research conducted by Qian [13], where Arizona Test Dust (ATD) was used for examination of the rate of surface particle resuspension (PR) resulting from an individual's walking and movement on three different surface materials. Previous studies have hardly considered the effects of the current around an individual, movement of the entire body, and type of ventilation. Tsai [14] investigated the variations in concentration due to particle resuspension from the garment in a clean room. A piece of fabric was placed in a container with a class-100 clean room. Although better, improved Lagrangian turbulence models have been provided, numerical research on particle movement in controlled spaces is conducted mostly using the Discrete Random Walk model. Aracena and et al. [15] performed experiments to determine the critical angular velocities of a particle on a rotating rough surface. Their experiments showed that the adhesion forces must be considered in forces balance of particle detachment. Benabed and et al. [16] experimentally studied human walking-induced particle resuspension in a full-scale chamber with two flooring types. This work revealed that the resuspension of PM1and PM2.5 is many orders of magnitude lower than PM10. Habchi et al. [17] investigated resuspension under the effect of transient flow using the DRW model. Kazzaz et al. [18] studied resuspension as influenced by oscillatory flow in a simple geometry.

Recently, Al Assaad et al. [19] studied developed a new empirically validated CFD modeling methodology for particle release from human skin and clothing in specific office settings. Ren [20] and et al. investigated experimentally the deposition of particles onto clothing and the resuspension of particles from clothing using a fluorescent-tracking technology.

As stated before, in previous studies of particle motion in controlled spaces, the importance of the turbulence dispersion models has not been addressed. Also, these studies mainly focused on the effect of the human walking on particulate matter sources in conventional ventilation systems, and less attention has been paid to the particles resuspension from the individual's body in unidirectional ventilation systems. In addition, the effect of isotropic and non-isotropic turbulence models on the resuspension and detachment of particles from surfaces has not been investigated.

So, the present paper attempts to fill the research gaps mentioned above. In this regard, the present research investigates the probability of particle resuspension from a garment in a controlled environment under vertical and horizontal unidirectional ventilation on an individual's body for different particle diameters to demonstrate the influence of flow direction and particle size. In addition, parameters such as particle density and

ventilation flow velocity are considered. For evaluation of the validity of different discrete-phase turbulence models with respect to particle size, isotropic and non-isotropic turbulence is studied, along with different particle turbulence dispersion models.
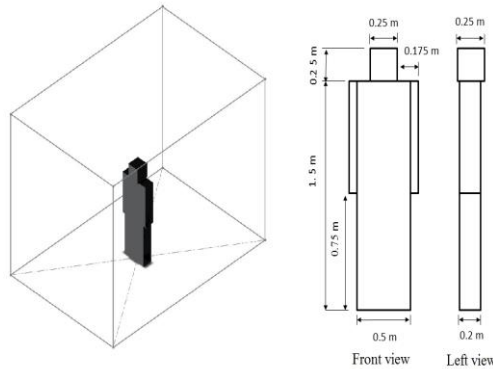
Figure 1. Left and front view of the user individual used in the simulation, along with schematics of the physical model (user in the room)

2. Physical model

The unidirectional ventilation room is the most common types of room, which can in turn be of the vertical or horizontal type. A unidirectional flow with a velocity of 0.3 to 0.45 m/s (the Reynolds number of 13000 to 20000) passes along the room in the controlled space simulated in this study [21]. This class-5 ISO clean room is 4 meters long, 2.7 meters wide, and 3 meters high. The intake and exhaust are considered here in two different arrangements: vertical unidirectional ventilation with a flow from the ceiling to the floor and horizontal unidirectional ventilation with a flow between two parallel walls.

Before entering the controlled space, the air passes through H13-class filters. The room is considered empty with no equipment present except the individual. The garment is assumed to be in compliance with the ISO-5 standard. The user's geometry and dimensions, as well as coordinates, are provided in detail in Figure 1. According to the figure, vertical unidirectional ventilation utilizes the entire ceiling as the flow air intake with exhausts on the floor, and horizontal unidirectional ventilation has its flow air intake facing the user, with the wall on the opposite side functioning as the air exhaust.

3. Mathematical description of the problem

In the analysis made in this research, air in standard conditions is used as the carrying fluid. According to the model geometry and flow characteristics in the present work, Reynolds number will be above 3750 which is resulted in passing turbulent flow through the user garment. It means that fluid velocity would be the sum of a mean and a fluctuating value at each point inside the field.

Several studies have been conducted so far to solve the problem of turbulent flow fields containing particles. Zhang and Chen [22] used the standard k-ε model in their investigation, which provided acceptable accuracy, but the results were far from those of experiments in some cases. As for deposition, Gao et al. [4] used three models, including k-ε RNG, k-ω SST, and Reynolds Stress Model (RSM), and concluded that k-ω SST and RSM provided better results. RSM calculates the amount of fluctuation in different directions, and is regarded as a non-isotropic model. Therefore, the present study uses RSM. Arizona Test Dust is used widely in investigation of aerosol distribution in clean spaces, so much so that standard high-efficiency filter tests are also conducted using the particles [13]. Over 70% of the ATD mass is silicon dioxide. In the present study, this material is used along with aluminum oxide to inspect particle resuspension from the garment surface. The characteristics of these materials are provided in Table 1, which are used for calculation of critical tension, required to resuspend the above particles.

Table 1. Characteristics of the Arizona Test Dust ingredients [2]

Material	ρ (10^3 kg/ m³)	K (10^{10} N/ m²)	W_A (10^{-3} N/ m²)	Mass percentage
SiO2	2.20	7.3	10.7	68-76
Al2O3	3.96	36	15.3	10-15

In the current study, particle density is assumed to be 2000 kg/m3, in accordance with previous studies [13].

3.1. Particle movement modeling

In the Lagrangian approach, particle behavior is regarded as a discrete phase, so the relevant equations should be analyzed separately in the reference coordinate system. The particle movement equation is Newton's second law, which is defined as Equation 1.

$$m_p \frac{du_p}{dt} = F_{fr} + F_g + F_b + F_s + F_{br} \qquad (1)$$

The right side of the equation represents the sum of the forces applied to the particle, including friction, gravity, buoyancy, Saffman lift, and Brownian. Friction is the main cause of the particles driving in and out of the room [23]. The friction force applied to the particle is similar to the drag force induced to a spherical particle in a laminar flow, which is calculated as Equation 2.

$$F_{fr} = \frac{1}{2C_c} C_d A_f \rho_f |u_r|^2 \qquad (2)$$

This force is in the same direction as particle and fluid relative velocity. The equation used for calculation of the drag coefficient is defined as Equation 3 [3].

$$C_d = \begin{cases} \dfrac{Re}{24} & Re_r \leq 1 \\ \dfrac{Re}{24}\left[1 + \dfrac{Re^{0.687}}{0.15^{-1}}\right] & 1 < Re_r \leq 1000 \\ 0.44 & 1000 < Re_r \end{cases} \quad (3)$$

C_c is Cunningham correction factor, and is obtained by Equation 4 [23]:

$$C_c = 1 + Kn\left(1.257 + 0.4exp\left(\frac{-0.55}{Kn}\right)\right) \quad (4)$$

where Kn is Knudsen number.

The gravity force induced to the particle is calculated by Equation 5.

$$F_g = \frac{\pi\rho_p d_p^3}{6}g \quad (5)$$

The buoyant force functions in the opposite direction of gravity, and is proportional to the volume of the object, carrying fluid density, obtainable from Equation 6.

$$F_b = -\frac{\pi\rho_f d_p^3}{6}g \quad (6)$$

F_{br} is the Brownian force. It is possible to demonstrate that the Brownian force can be modeled as white noise, a random even parameter with Gaussian distribution and zero average. White-noise spectrum intensity is described by Equation 7 [25]:

$$S_{nn} = \frac{2k_B T\beta}{\pi m_p} \quad (7)$$

where β is the particle velocity factor in the Lagrangian equation ($du/dt + \beta u = n(t)$), T is temperature (in Kelvin), and k is Boltzmann constant. The amount of the Brownian force can be obtained from Equation 8 [26].

$$n(t_i) = G_i\sqrt{\frac{\pi S_{nn}}{\Delta t}} \quad (8)$$

The presence of velocity gradient in the continuous phase induces a lift force to the particle, which is known as the Saffman lift, defined by Equation 9 [27].

$$F_s = 1.61\rho_f v_f^{\frac{1}{2}} d_p^2|\nabla \times \vec{u}_f|^{\frac{-1}{2}}[(\vec{u}_f - \vec{u}_p)](\nabla \times \vec{u}_f) \quad (9)$$

Some parameters need to be defined for studying and solving the movement of particles, one of the most important being particle relaxation time, obtained in Stokes regime by Equation 10.

$$\tau_r = \frac{\rho_p d_p^2 C_c}{18\mu_f} \quad (10)$$

Another noteworthy parameter, also used in Lagrangian turbulent section equations, is particle terminal velocity, i.e., velocity of freefalling under the influence of gravity, obtained in Stokes regime, which is calculated by Equation 11.

$$V_{ter} = \frac{g d_p^2 C_c}{18\mu_f}(\rho_p - \rho_f) \quad (11)$$

3.2. Evaluation of discrete phase turbulence

Turbulent fluid flow and velocity fluctuations directly affect particle movement, where the instantaneous velocity felt by the particle changes due to the changes in the forces applied to it. Velocity fluctuates randomly in a turbulent flow, where each particle experiences different velocities at the same spot at different times. Several methods have been proposed for indicating the effect of turbulence in the particle movement equation. The five methods used in this study are introduced below.

3.2.1. Discrete Random Walk

The best-known method of modeling continuous phase velocity fluctuations is the Discrete Random Walk method. Its greatest feature is that it samples particle velocity fluctuations with Gaussian distribution, zero average, and mean variance equal to the root mean square of the turbulent velocity fluctuation, which are calculated by Equation 12 and 13. In this sampling method, the fluctuating velocity is kept constant in a time interval corresponding to the time scale of vortices. In non-isotropic conditions, Reynolds stress components (u'^2, v'^2, w'^2) are directly used [28] .

$$\sqrt{u'^2} = \sqrt{v'^2} = \sqrt{w'^2} = V_{rms} = \sqrt{\frac{2k}{3}} \quad (12)$$

$$u_f = \left(\bar{u} + \xi\sqrt{u'^2}\right)\hat{\imath} + \left(\bar{v} + \xi\sqrt{v'^2}\right)\hat{\jmath} + (\bar{w} + \xi\sqrt{w'^2})\hat{k} \quad (13)$$

where ξ represents a random number with Gaussian distribution. A Gaussian distribution is defined with an average value and a standard deviation, which are 0 and 1 here, respectively. Thus, fluid velocity in the movement equation is as shown in Equation 13.

In the analysis procedure, the above random number changes in accordance with the turbulence field. The change is specified given the length scale of the eddy and the time it takes the particle to cross it. The lifetime of the eddy is determined by Equation 14:

$$\tau_e = 2T^L \quad (14)$$

where T^L is the Lagrangian integral time scale of the particle, calculated by Equation 15.

$$T^L = C_L \frac{k}{\varepsilon} \qquad (15)$$

C_L is assumed to be 0.3, and particle crossing time is obtained by Equation 16:

$$t_{cross} = -\tau_r ln\left[1 - \left(\frac{l_e}{\tau_r|\vec{u} - \vec{u}_p|}\right)\right] \qquad (16)$$

where τ_r is particle relaxation time, and le is eddy length scale, calculated by Equation 17 [29].

$$l_e = 0.165\frac{k^{3/2}}{\varepsilon} \qquad (17)$$

In the discrete random walk method, the particle interacts with the turbulent field either while it crosses the eddy, or until the eddy dies out; therefore, the time of interaction of the particle with the turbulent field is the smaller duration.

3.2.2. Fourier-Kraichnan method [30]

Kraichnan presented a simple method that creates a random field similar to pseudo-isotropic turbulence. Having studied turbulence simulation using the fluid energy spectrum function, he suggested an idea for fluid velocity fluctuations, and measured the fluid energy spectrum. In this method, fluid velocity fluctuations are calculated using Equations 18, 19, and 20 [30, 31], applicable in incompressible conditions.

$$\vec{W}_f(\vec{X}_p, t)$$
$$= \sqrt{\frac{2}{N}}\left[\sum_{n=1}^{N} \vec{u}_1(\vec{k}_n).cos(\vec{k}_n.\vec{X}_p + \omega_n t) + \vec{u}_2(\vec{k}_n).sin(\vec{k}_n.\vec{X}_p + \omega_n t)\right] \qquad (18)$$

$$\vec{u}_1(\vec{k}_n) = \vec{\xi}_n \times \vec{k}_n, \vec{u}_2(\vec{k}_n) = \vec{\zeta}_n \times \vec{k}_n \qquad (19)$$

$$\vec{k}_n.\vec{u}_2(\vec{k}_n) = \vec{k}_n.\vec{u}_1(\vec{k}_n) = 0 \qquad (20)$$

in these equations, ξ_n, ζ_n, and ω_n (frequency value) are acquired independently from Gaussian distribution. Each of the k_n parameters is a random Gaussian value with a standard deviation of 0.5, which is considered as a function of the energy spectrum, and n is the number of utilized series, which is usually 100.

Nondimensional values are described by Equation 21.

$$\vec{X} = \frac{\vec{x}}{l_0}, t^* = \frac{t}{t_0}, \vec{W}_f = \frac{\vec{u}'}{\sqrt{\vec{u}'^2}} \qquad (21)$$

where l_0 and t_0 are factors of flow and geometry, and W_f represents nondimensional fluid phase velocity fluctuations.

3.2.3. Model based on Langevin equation

In this model, benefitting from Langevin equation, the relation and correlation between the fluid and the particle (Eulerian) is recognized by Frenkiel family of exponential functions, and the correlation between particle velocity and its history is acquired by the Langevin equation (Equation 22).

$$du = u(t + dt) - u(t) = -\frac{u}{T_L} + \sigma_f \sqrt{\frac{2}{T_L}} dW \qquad (22)$$

Here, dW is Wiener Process (white noise) which averages zero (<dW>=0), and time interval equals variance (<(dW)²>=dt). The advantage of using this formula is that it provides better physical compatibility. Berlemont et al. [32] proposed an innovative extension of discrete Langevin formula, utilized below. It is not simply a proposed discretization derived for a correlation function but rather a continuous model found on a random differential equation, resulting in the real form of correlation. The discretization of the equation is formulated as Equation 23:

$$u^{n+1} = au^n + b\xi^n \qquad (23)$$

where ξ is a random number obtained from normal Gaussian distribution.

The equation is valuable in that it focuses on the main physical idea of the model, and materializes it. Fluid velocity is given in a certain t_n time frame, and is determined in the next time frame $t^{n+1}=t^n+\Delta t$ by the sum of the predefined values of a phrase containing the memory of the previous velocity and a random phrase for acceleration fluctuations.
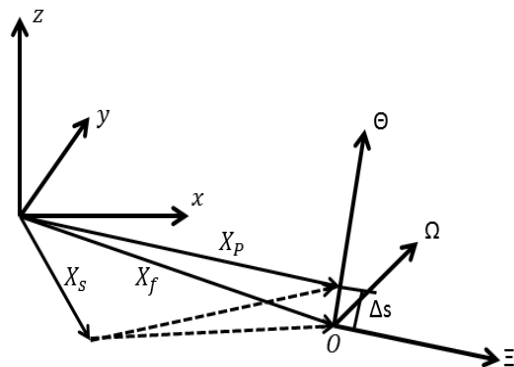
Figure 2. Particle and fluid point position
at moments t and t+Δt

To obtain the values of the a and b coefficients, the above equation is multiplied by u^n and u^{n+1}, and the mean result is calculated from Equations 24 and 25.

$$a = \frac{\langle u^n u^{n+1}\rangle}{\langle(u^n)^2\rangle} = R_L(\Delta t) = exp\left(-\frac{\Delta t}{T_L}\right) \qquad (24)$$

$$b = [\langle u^{n+1}u^{n+1}\rangle - a^2\langle(u^n)^2\rangle] = (1 - a^2)\sigma_f^2 \qquad (25)$$

Subsequent use of the exponential correlation in steady state results in Equation 26.

$$\langle(u^n)^2\rangle = \sigma_f^2 \qquad (26)$$

3.2.4. Lagrangian Temporal Construction Model (LTCM)

Lu et al. [33] presented a new model with better compatibility with experimental results. This method is based on Lagrangian correlation of random particle movement from X_s to X_f.

The fluid point and the particle are assumed to be at the same position (X_s) at moment t, and reach positions X_f and X_p, respectively, after a time step (Δt). The distance between these two is shown in Figure 2 as Δs. The local coordinates $0 - \Theta\Xi\Omega$ are defined by particle movements. X_f, X_s, and X_p are located at the original coordinates. In the first step of LTCM, particle position and velocity at moment zero are given, and the initial fluid fluctuations are then obtained through the Discrete Random Walk model. In the second step, the fluid point position at X_f is calculated by the velocity differential equation.

The particle position X_p is acquired through momentary velocity and the particle movement equation. All the values required for formation of a local system of coordinates are thus obtained. once that step is taken, a return is made to the second step, where the acquired location data are set, and the fluctuation velocities in the local system of coordinates are calculated. Afterwards, the local coordinates need to be converted to the original ones, and the new value of velocity is used to set initial velocity.

According to Equations 27 and 28 the relations between particle velocity fluctuations in the initial and secondary positions are calculated in LTCM model.

$$W_i(X_p) = a_i b_i W_i(X_s) + \psi \qquad (i = 1,2,3) \qquad (27)$$

$$\psi_i = \sqrt{1 - (\alpha_i b_i)^2} \qquad (28)$$

Frenkiel proposed the following forms (Equations 29 and 30) of temporal and local correlation functions for α_i and b_i.

$$\alpha_i = exp\left(\frac{-\Delta t}{T_i^L}\right) \qquad (29)$$

$$b_i = exp\left(\frac{-\Delta s}{2\Lambda_i}\right) cos\left(\frac{\Delta s}{2\Lambda_i}\right) \qquad (30)$$

These functions use length scales, where Λ_1 is the longitudinal scale, and Λ_2 and Λ_3 are the transverse ones, as estimated Equations 31 and 32 [33].

$$\Lambda_1 = 2.502 T_i^L \sqrt{\overline{u^2}_\iota} \qquad (31)$$

$$\Lambda_2 = \Lambda_3 = 0.5\Lambda_1 \qquad (32)$$

3.2.5. Langevin-Lagrangian Temporal Construction Model (L-LTCM)

This method is a mixture of Langevin and Lagrangian Time Construction Models. The definition of this method is similar to that of Lagrangian Time Construction Model, different in that Langevin equation is used here instead of Eulerian correlations. As in the coefficient acquired in the Langevin Equation 25 is used in Equation 28 and Equation 33 [34].

$$\psi = (1 - a^2)\sigma_f^2 \xi^n \qquad (33)$$

4. Resuspension

A physical process through which a particle is detached from the surface. It usually occurs due to aerodynamic forces created by the shear flow. In this study, an improved version of the Johnson-Kendell-Roberts model [35] is used to simulate particle resuspension under an applied shear tension.

Furthermore, Soltani and Ahmadi [36] extracted an analytical model to predict particle surface detachment, and referred to rolling as the most probable mechanism of spherical particle resuspension from real surfaces. Therefore, the shear tension velocity required for particle detachment is as follows (Equation 34).

$$u_c^* = \left[\frac{a^2 C_C f_{po} \, exp\left(-\frac{0.6}{A_c^2}\right)}{2.52\rho d_p^3}\right]^{1/2} \qquad (34)$$

If shear velocity is higher than the above value, the particle qualifies for detachment. However, it should be observed whether the particle enters the main flow, or is deposited. For evaluation of the effects of the air flow around an individual over the particle surface, resuspension rate and resuspension probability are defined as Equations 36 and 37, respectively [12, 37].

$$PR = \frac{N_R}{N_L} \qquad (35)$$

$$RR = \frac{R}{L} = \frac{PR}{T_r} \qquad (36)$$

$$C = \frac{N_R}{V} = PR \times \frac{L \times A}{V} \qquad (37)$$

In Equation 35, particle resuspension probability is the proportion of the number of particles resuspended from the surface (NR) to the number of particles present on the surface (NL), and resuspension rate (RR) is the proportion of resuspension flux (in particles per second per cubic meter) to particle load (L) on the surface (in particles per cubic meter), according to Equation 36. Particle resuspension rate can be obtained based on the probability of particle resuspension, which is the proportion of resuspension probability to resuspension time. rate is the significant parameter for distribution of particles with different diameters, as also explored in the present research.

4.1. Lagrangian analysis of particle resuspension

There are particles on the surface, which are detached given the appropriate circumstances. Focused on previously in the section on detachment, the circumstances provide the critical shear velocity on the surface. The flow around the surface determines the value of shear velocity thereon, and the particle is detached from the surface if it rises to a value higher than critical shear velocity. It then moves, either returning to the surface and resettling, or entering the main flow and being removed from the calculation zone. In this method, particles are observed from the source, i.e., the surface, and the computational cost of the procedure is thus significantly lower than when the particle is followed in the entire room space.

4.2. Mesh and number-of-particles independence studies

4.2.1. Mesh independence study

After evaluation of the model, a mesh of appropriate density needs to be chosen to prevent the results from dependence on the one selected for the studied case. In this regard, according to Figure 3, a three-dimensional
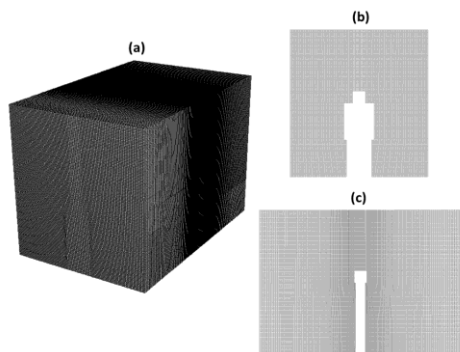
Figure 3. A typical structured grid of the physical model geometry: (a) three-dimensional view, (b) front view, and (c) side view

structured grid of the physical model geometry has been generated in Gambit software. For investigation of the mesh independence of the results, meshes with 590920, 980000, 1892000, and 2860000 cells are examined. Figure 4 shows vertical velocity over the line created on Figure 1 for different numbers of cells. Clearly, no significant changes are observed in the simulation results as the number of cells is increased from 1892000 to 2860000. Therefore, the 1892000-cell mesh is selected for the simulation.

4.2.2. Number-of-particles independence study

The computational cost of Lagrangian analysis is directly proportional to the number of particles used in the analysis. Therefore, it is highly desirable to reduce the number of particles as far as possible to save up run time. However, the number of particles should not be lower than the minimum number of particles required for accurate results.

Presence of a random number in the DRW algorithm and other models changes PR. After mesh independence is studied, therefore, independence from the number of particles present on the unit of area that are tracked for rising should be studied.
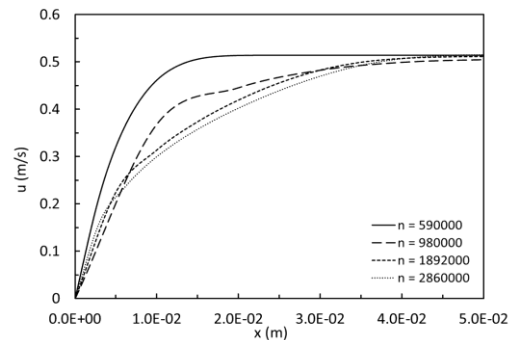
Figure 4. Vertical velocity mesh independence study
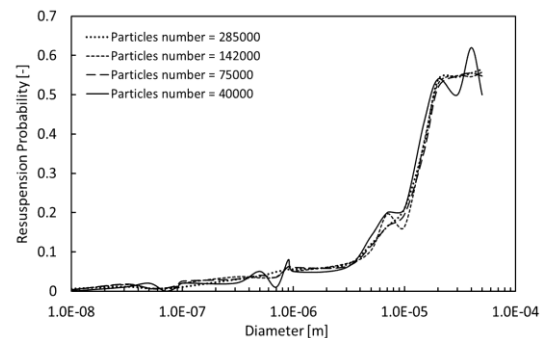
Figure 5. Study of independence from the number of particles for the probability of particle resuspension from the garment

Figure 5 shows independence from the number of released particles for calculation of the probability of particle resuspension from the user's garment in a vertical unidirectional system with an entrance velocity of 0.5 m/s (Langevin model). 142000 is found to be the appropriate number of particles on the garment to be exposed to the incoming flow.

4.3. Boundary conditions

In the fluid hase, the inlet boundary condition of the room is the velocity inlet, where the velocity varies from 0.3 to 0.45 m/s. The outlet boundary condition is the outflow, and no-slip boundary conditions are adopted at the room walls and garment. In the discrete phase, the escape type boundary condition is assumed at the inlet and outlet of the room. The reflect boundary condition is imposed for particles collide with the walls and garment. At the walls, the reflect boundary with a restitution coefficient of 1 is used. As stated before, the resuspension boundary condition is applied through comparing the shear velocity with the value of relation (34). Table 2 lists the boundary conditions used in the present work.

Table 2. Boundary conditions of governing equations

	Room walls	Room inlet	Room outlet	Garment
Fluid phase				
velocity	no slip	velocity inlet	outflow	no slip
pressure	zero gradient	-	atmospheric pressure	zero gradient
Discrete phase				
	reflect	escape	escape	reflect & resuspension
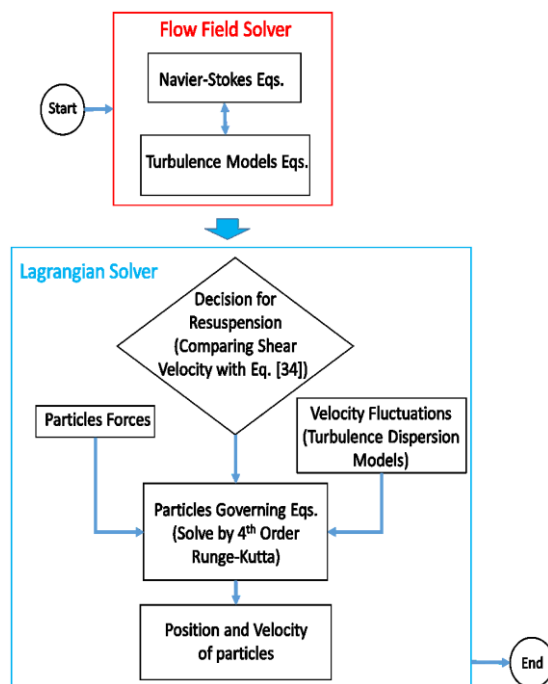
Figure 6. Solution algorithm of the governing equations in the present work

4.4. Solution method

In this study, FLUENT software has been utilized to solve the flow field governing equations. A three-dimensional steady-state numerical simulation has been conducted by using the finite volume method. In this method, the SIMPLE algorithm was used for the velocity-pressure coupling. The second-order upwind and the central-difference discretization schemes were applied for convective and diffusive terms, respectively. The convergence criteria for the flow field were controlled by the maximum residual level of 1e-5 for each governing equation and 1e-3 for the maximum net mass flow rate between inlet and outlet. In this work, the effect of the particles on the fluid was ignored. Hence, first of all, the governing equations of flow field were solved and the flow information was then used in the Lagrangian solver. In the Lagrangian solver, at first, the amount of all forces applied to the particles were calculated and then the flow velocity fluctuations were modeled with the aid of the

aforementioned turbulence dispersion models. Finally, Lagrangian equations were directly solved by the fourth order Runge-Kutta method and then the position and velocity of the particles in the flow field were calculated. The detail of the solution algorithm is presented in Figure 6.

5. Results

In this section, the validity of the turbulence dispersion models is conducted against the experimental data. Then, the simulation of particle resuspension and the effect of isotropic anisotropy on this phenomenon in the horizontal unidirectional ventilation system are being investigated. In the next step of the simulation, turbulence dispersion in horizontal and vertical unidirectional systems on particle resuspension probability is studied. Finally, turbulence dispersion models' evaluation is performed in terms of the accuracy and computational speed.

5.1. Model validation

Before the analysis is made, it is vital to evaluate the developed code and selected models. For this purpose, experimental data are taken from Tsai [14], focused on particles released from a piece of polyester fabric in an ISO-5 clean room in steady-state conditions and reporting particles of 10 to 0.01 microns. The rectangular piece of fabric with dimensions of 0.147*0.179 meters was placed in a box with a volume of 1400 cm3. The unidirectional flow in the container passed from a side wall to another at 0.15 m/s.

In this section, Tsai's [14] experimental research is simulated numerically, and the findings are analyzed. The sources of particles in the clean room include only the piece of fabric and the unidirectional ventilation system. The concentration diagram obtained from the experimental data can thus be compared to the particle resuspension probability diagram. RSM is used to simulate fluid flow turbulence. With particle load (L) on the polyester surface assumed to be as in Equation 38, the concentration in the room is calculated using Equation 37.

$$L = 2.527 \times 10^7 D \qquad (38)$$

Figure 7 depicts the numbers of particles with different diameters per unit of volume in the class-100 clean room, on which basis the concentration of particles with diameters below 0.6 microns is nearly zero, followed by a relative maximum. An important finding is that the particle distribution behavior based on particle diameter in clean rooms is a function of particle resuspension probability, an effective factor in particle concentration. Consequently, the resuspension probability parameter is useful in investigation of particle resuspension and concentration in controlled spaces.

It is clear from Figure 7 that the distribution models have an acceptable trend in specification of concentration, and that all the models predict the rise in probability similarly to the concentration diagram generated from experimental results. Due to the micron-sized particles considered in this section, the difference in prediction of resuspension probability by different models is minimal.
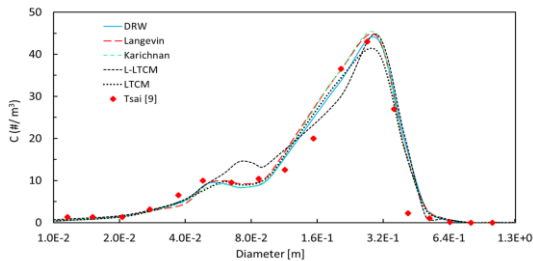
Figure 7. Concentration of particles with different diameters

In terms of computational cost and accuracy, DRW can be considered as an appropriate model for particles in a clean room with diameters in the above range. This diameter range is common for a controlled-space study, but a wider range is considered in this research for investigation of model predictions.

At the moment a particle rises from a horizontal surface, Saffman force is strongly applied to it in the opposite direction of the rise due to velocity gradient close to the surface. Saffman force is directly proportional to d_p^2. Therefore, the larger the diameter, the greater the force opposing the rise. Simulation shows that flow hydrodynamic forces overcome the particle at 0.6 microns. The trend continues up to the maximum resuspension. The flow force is applied to the particle through the friction force (i.e., drag), and is proportional to d_p^3. After the peak, the force decreases, and particle resuspension from the surface recedes as a result. As the trend continues, it becomes highly unlikely for particles with large diameters to be resuspended from the surface.

5.2. Particle resuspension in a vertical unidirectional ventilation system

This section explores the predictions of turbulence dispersion models on the probability of particle resuspension from a user's body in a vertical flow from ceiling to floor. It should be noted that air flow is predicted by the RSM model. Commonly, flow velocity ranges between 0.3 and 0.5 m/s. The air velocity in the clean room is first assumed to be 0.5 m/s, and the effects of velocity, particle density, and isotropic turbulence are then studied.

According to the resuspension probability trend in Figure 8, it is possible to split the diagram to three sections. The dominant forces are drag and gravity in the first section (Section 1), drag and Brownian in the middle section (Section 2), and the Brownian force in

the final section (Section 3). The general trend of prediction suggests that particles with diameters of above 5 microns have a high probability of rising, and ones with diameters of above 20 microns have high chances of being removed from the garment. This trend has also been observed in experimental studies for particle resuspension [14, 16] which is due to the general trend of probability.
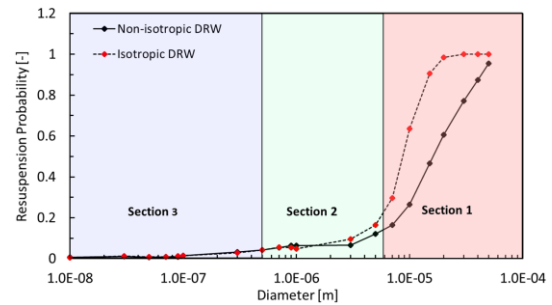
Figure 8. Probability of particle resuspension from the user's garment in a vertical unidirectional ventilation system at a velocity of 0.5 m/s provided by two DRW models

Figure 8 shows the difference between the effects of isotropic and non-isotropic flow on the particles in the drag force dominance region for particles with perpendicular to the surface are calculated more profoundly, which helps particle rising; for sub-micron particles, however, which are influenced more severely by the Brownian force, the isotropic or non-isotropic nature of the turbulence exhibits little effect. Another reason is that the drag forces, which transfer flow turbulence effects to the particle, are significantly less effective at lower diameters. While the isotropic DRW model predicts this, the isotropic and non-isotropic DRW models provide essentially similar simulations for sub-micron particles. Kraichnan model simulates the fluctuations more acutely against DRW, and more particles in wide diameter ranges are therefore resuspended with higher resuspension probability.
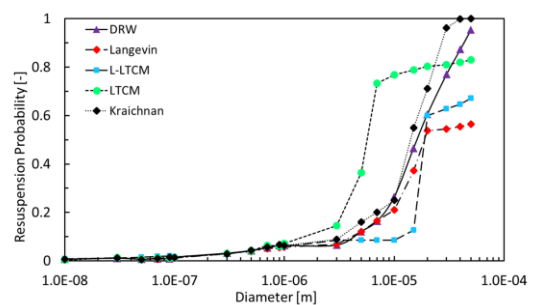
Figure 9. Probability of particle resuspension from the user's garment in a vertical unidirectional ventilation system at a velocity of 0.5 m/s provided by different dispersion models

As a general rule, self-correlating models such as Langevin, LTCM, and L-LTCM predict similar behavior. According to the correlation coefficients, there are

variations in the simulation of these models, as evident in Figure 9. The vertical unidirectional system simulations demonstrate that the system causes particles with diameters of 5 microns or above to rise, and greatly increases their concentration in the environment. Therefore, garment and underwear designed for rooms with this type of ventilation should generate fewer particles of the above size range.

5.2.1. Effects of velocity on particle resuspension

This section explores the effects of velocity on particle resuspension in a vertical unidirectional ventilation system examined using DRW. The fluid flow around the user is simulated at three different velocities (0.3, 0.4, and 0.5 m/s), and the DRW model is then used.
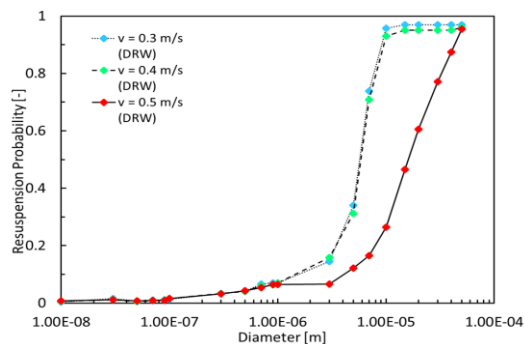
Figure 10. Probability of particle resuspension from the user's garment in a vertical unidirectional ventilation system for different velocities examined with the DRW model

As seen in Figure 10, the probability of resuspension of large particles and their concentration in the clean space increases as unidirectional ventilation velocity decreases. The above decrease exhibits little effect on the probability of resuspension of small particles. Another cause of concern is that particle concentration rises on a broader scale as velocity decreases, which requires preparations. From a physics point of view, the rise results from the lower velocity gradient on the surface and the subsequent decrease in the Saffman force opposing particle rising.

5.2.2. Effects of density on particle resuspension

For examination of the effects of density in particle rising, aluminum oxide particles are simulated, and the results are compared to those concerning silicon dioxide particles.

Possible resuspension probability is shown in Figure 11 for the two materials. Clearly, particle resuspension grows as density increases for diameters of over one micron due to the gravity force, which causes the great increase in resuspension rate for larger diameters by helping the particle to get detached from the surface. On average, a 10% increase is observed in resuspension for a growth only by 80% in density.
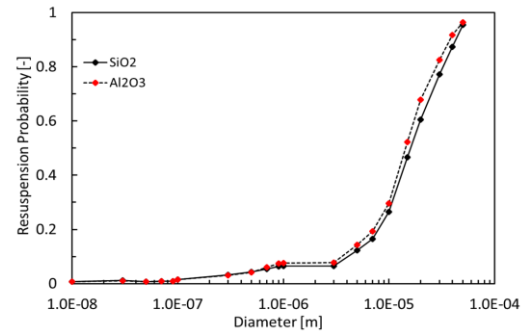
Figure 11. Probability of silicon dioxide and aluminum oxide particle resuspension from the user's garment in a vertical unidirectional ventilation system examined with the DRW model

The results demonstrate how changes in density affect particle resuspension against diameter. For particles with diameters smaller than one micron, there is a small recession in resuspension probability due to the decrease in Brownian distribution, explained by the less energy received by higher-density particles as a result of the fluid molecules.

5.3. Particle resuspension in a horizontal unidirectional ventilation system

This section reviews the predictions made by particle turbulence dispersion models on the probability of particle resuspension from a user's garment under a horizontal flow. The flow surrounding the individual is simulated by the RSM model. Ventilation intake flow velocity is assumed to be 0.25 m/s. The effects of velocity on particle resuspension are examined below.

The particle resuspension procedure in a horizontal ventilation system is similar to that in a vertical system, but eddies take shape around the user in a horizontal system, which makes them more effective on resuspension of smaller particles, so particles of a wider range of sizes enter the system. Moreover, the probability of resuspension and deposition of particle cycles is high in a horizontal ventilation system. On the other hand, a larger particle, with a higher probability of resuspension in a vertical ventilation system, has a lower chance of resuspension in a horizontal one due to the same direction of the flow and the gravitational force.

With the walking individual's leg movements neglected, his presence can be considered similar to that of a moving individual in a clean room, or to flow with different relative velocities in the direction of horizontal ventilation. Therefore, particle resuspension probability is an expression of particle resuspension for a moving individual in such a ventilation system.

Figure 12 depicts the DRW predictions for particles of different diameters resuspended from a user's garment in a horizontal ventilation system with a flow velocity of 0.25 m/s.
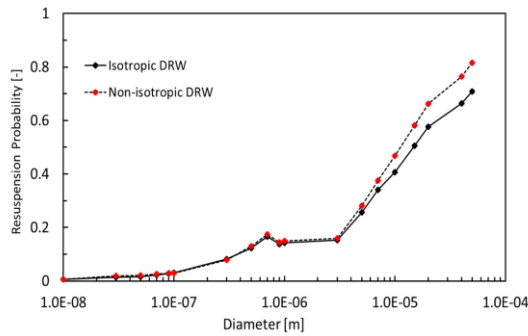
Figure 12. DRW predictions on particle resuspension from the user's garment in a horizontal ventilation system with a current velocity of 0.25 m/s

The model anticipates a 25% chance of resuspension for particles with diameters of over 5 microns, and 15% for 0.5- to 5-micron particles, while resuspension probability for a similar velocity in a vertical system is predicted to be 97% for particles larger than 5 microns in diameter and below 8% for particles smaller than 5 microns. The isotropic DRW model exhibits similar predictions for particles with diameters smaller than 5 microns, while there is discrepancy and divergence for larger particles, resulting from the more profound effect of Brownian motion and lower influence of turbulence. The results indicate the tendency of the horizontal system to rise more particles with diameters between 0.5 and 5 microns and induct them in a clean room. This is an important range, as filters exhibit the lowest efficiency in removal of particles with diameter sizes lying therein. For example, bacteria, which are detrimental to clean rooms used in medical and pharmaceutical applications, are categorized as such particles.

5.3.1. *Effects of velocity on particle resuspension*

Figure 13 shows the probability of particle resuspension from a user's garment at different velocities using the DRW model. Unlike in the vertical system, velocity is directly proportional to particle resuspension probability here. Due to the intensifying effect of the flow on the eddy surrounding the user's body, more particles are detached from the garment surface to enter the main flow.
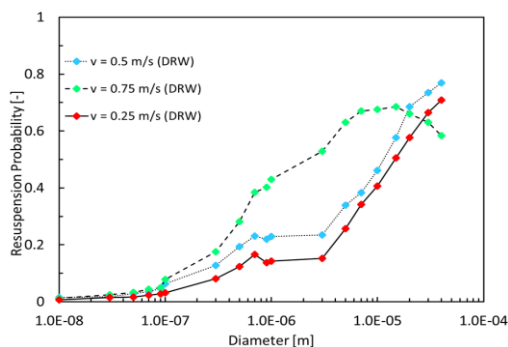
Figure 13. Probability of particle resuspension from the user's garment for different velocities in a horizontal unidirectional ventilation system examined using the DRW model

Moreover, a horizontal system releases a wide range of particles into the controlled space, while resuspension probability is lower in a horizontal system than in a vertical one.

5.3.2. *Models evaluation*

According to Table 3, all implemented turbulence dispersion models in the present work were compared through three characteristics, including: 1. simulation accuracy for particles size below 0.6 microns, 2. simulation accuracy for particles size above 0.6 microns, and 3. computational speed. In general, in term of computational accuracy, Langevin and L-LTCM models have the highest and lowest accuracy in resuspension probability prediction, respectively. In term of computational speed, the highest and lowest accuracy respectively belong to DRW and Fourier-Kraichnan models. Finally, it can be claimed that Langevin model has the highest performance compared to other models. Computational speed is very important for simulation in the Lagrangian approach. According to the results, calculation speed of the Langevin model ranks second among the models; but its computational speed is acceptable in comparison with other models. Consequently, Langevin model is recommended as an appropriate turbulence dispersion model to simulate particle motion in controlled spaces.

Table 3. The comparison of the turbulence dispersion models performance implemented in the present study

Characteristic	Models				
	DRW	Fourier-Kraichnan	Langevin	LTCM	L-LTCM
Simulation accuracy for particles size below 0.6 microns	✗	✓✓	✓✓✓	✓	✗✗
Simulation accuracy for particles size above 0.6 microns	✓✓	✓✓	✓✓	✓✓	✗✗
Computational speed	✓✓✓	✗✗	✓✓	✓✓	✓

Guide: ✓✓✓ excellent, ✓✓ very good, ✓ good,
✗ weak, ✗✗ too weak

6. Conclusion

In this study, particle resuspension probability was introduced for controlled space ventilation systems, and it was then inspected using different particle turbulence dispersion models. Notable results obtained from the present study can be listed as below:

- Increasing flow rate and velocity in a vertical ventilation system decreases particle rising,

while converse behavior is observed in a horizontal system. At the same velocities, a horizontal unidirectional ventilation system resuspends more particles with diameter sizes between 0.1 and 10 microns, which are more difficult to remove from the system using filters.

- Rooms with horizontal ventilation systems require higher standards of user garments for the same cleanness class.

- Due to the decreasing turbulence effects and increasing Brownian influence (close to the walls), most models offer similar performance for particles of sizes less than one micron.

- The resulting discrepancy between the self-correlating and the Kraichnan and DRW models grows as velocity or diameter size increases.

- The assumption of isotropic turbulence is not appropriate for particles with diameters of over one micron.

- Employment of non-isotropic turbulence models is quite significant in distribution of particles with diameters of 10 microns or above, so such fluid flows should be simulated by non-isotropic turbulence models.

- Langevin model has the highest performance compared to other models in term of computational speed and accuracy.

Nomenclature

a	Contact radius [m]
A	Garment area [m²]
A_f	Particle forehead area [m²]
C	Concentration [kgm⁻³]
C_c	Cunningham slip correction factor [#m⁻³]
C_d	Drag force factor
C_L	Heat driving force velocity [ms⁻¹]
d	Diameter [m]
dW	White Noise function
F	Particle induced force [N]
f_{po}	Separation force [N]
g	Gravitational acceleration vector [ms⁻²]
G_1, G_2	Gaussian numbers [kgs⁻¹]
J	Wall particle flux [kgs⁻¹]
k	Turbulent kinetic energy, Boltzmann constant [m²s⁻², JK⁻¹]
k_B	Boltzmann constant [JK⁻¹]
K	Yang complex coefficient [Nm⁻²]
Kn	Knudsen number

k_n	Gaussian numbers
l_e	Eddy length scale [m]
l_0	Length scale of physical model [m]
L	Particle concentration on the surface [#m⁻²]
m	Mass [kg]
N_d	Number of deposited particles [#]
N_L	Particle number on the surface [#]
N_R	Number of Resuspended particles [#]
N_0	Initial number of particles [#]
PR	Resuspension Probability
R	Resuspension flux [#s⁻¹m⁻²]
R_E	Eulerian correlation
R_L	Lagrangian correlation
Re	Reynolds number
RR	Resuspension rate [s⁻¹]
s_{nn}	White noise intensity spectrum
t	Time [s]
t_d	Deposition Time [s]
t_0	Time scale [s]
t_d^+	Nondimensional time duration
t^*	Nondimensional time
t_{Cross}	Particle crossing time [s]
t_{int}	Particle-eddy interaction time [s]
T	Absolute temperature [K]
T_r	Resuspension time [s]
T_i^L	Particle lagrangian integral time scale [s⁻¹]
u	X-aligned velocity [ms⁻¹]
$\vec{u}$	Velocity vector [ms⁻¹]
$\bar{u}$	Mean velocity [ms⁻¹]
u'	Fluctuations Velocity [ms⁻¹]
u^*	Shear velocity [ms⁻¹]
u_r	Relative particle-fluid velocity [ms⁻¹]
v	Y-aligned velocity [ms⁻¹]
V	Room volume [m³]
V_d	Deposition velocity [m³s⁻¹]
V_d^+	Nondimensional deposition velocity
V_{ter}	Terminal velocity [ms⁻¹]
w	Z-aligned velocity [ms⁻¹]
W	Nondimensional velocity fluctuation
W_A	Adhesion thermodynamic work [J]
$\vec{x}$	position Vector [m]
$\vec{X}$	position [m]
$\vec{X}$	Nondimensional position Vector

y_0	Length of injected particle[m]
y_0^+	Nondimensional length of injected particle
β	Mobility coefficient [º]
Δ_c	Nondimensional roughness
ε	Turbulent Energy Dissipation Rate [m^2s^{-3}]
ζ	Gaussian Random Number
μ	Fluid Dynamic Viscosity [$kgm^{-1}s^{-1}$]
ν	Fluid Kinematic Viscosity [m^2s^{-1}]
ξ	Gaussian Random Number
Λ	Eulerian length scale [m]
ρ	Density [kgm^{-3}]
σ	Velocity variance [ms^{-1}]
τ_d	Nondimensional Particle Relaxation Time
τ_e	Lifetime of eddy [s]
τ_r	Particle Relaxation Time [s]
ω	Frequency velocity fluctuations in Fourier [s^{-1}]
b	Buoyancy
br	Brownian
f	Fluid
fr	Drag
g	Gravity
p	Particle
r	Relative
s	Saffman

Acknowledgements

References

[1] Mouritz, A.P., Gellert, E., Burchill, P. and Challis, K., 2001. Review of advanced composite structures for naval ships and submarines. *Composite structures*, *53*(1), pp.21-42.

[2] Zhang, X., Ahmadi, G., Qian, J., & Ferro, A. 2008. Particle detachment, resuspension and transport due to human walking in indoor environments. Journal of Adhesion Science and Technology, 22(5-6), pp.591-621.

[3] Tian, L., & Ahmadi, G. 2007. Particle deposition in turbulent duct flows—comparisons of different model predictions. Journal of Aerosol Science, 38(4), pp.377-397.

[4] Gao, N., Niu, J., He, Q., Zhu, T., & Wu, J. 2012. Using RANS turbulence models and Lagrangian approach to predict particle deposition in turbulent channel flows. Building and Environment, 48, pp.206-214.

[5] Mito, Y., & Hanratty, T. J. 2002. Use of a modified Langevin equation to describe turbulent dispersion of fluid particles in a channel flow. Flow, turbulence and combustion, 68(1), pp.1-26.

[6] Kang, Y., Wang, Y., & Zhong, K. 2011. Effects of supply air temperature and inlet location on particle dispersion in displacement ventilation rooms. Particuology, 9(6), pp.619-625.

[7] Kubota, Y., Hall, J. W., & Higuchi, H. 2009. An experimental investigation of the flowfield and dust resuspension due to idealized human walking. Journal of fluids engineering, 131(8).

[8] Khalifa, H. E., & Elhadidi, B. 2007. Particle levitation due to a uniformly descending flat object. Aerosol science and technology, 41(1), pp.33-42.

[9] Zheng, S., Du, W., Zhao, L., & Zhang, J. 2018. Simulation of Particle Resuspension Caused by Footsteps. Environmental Processes, 5(4), pp.919-930.

[10] Boulbair, A., Benabed, A., Janssens, B., Limam, K., & Bosschaerts, W. 2022. Numerical study of the human walking-induced fine particles resuspension. Building and Environment, 216, p.109050.

[11] Sun, Z., Zheng, S., Fu, Y., & Chai, M. 2022. Characteristics of indoor human-induced particle resuspension under different ventilation conditions. Indoor and Built Environment, p.1420326X221084032.

[12] Sajadi, B., Saidi, M. H., Ahmadi, G., Kenney, S. M., & Taylor, J. 2013. On the induced airflow and particle resuspension due to a falling disk. Particulate Science and Technology, 31(2), pp.190-198.

[13] Qian, J., Peccia, J., & Ferro, A. R. 2014. Walking-induced particle resuspension in indoor environments. Atmospheric Environment, 89, pp.464-481.

[14] Tsai, C. S. J. 2015. Contamination and release of nanomaterials associated with the use of personal protective clothing. Annals of Occupational Hygiene, 59(4), pp.491-503.

[15] Aracena, K. D. L. Á. V., Uñac, R. O., Ippolito, I., & Vidales, A. M. 2020. Movement initiation of millimeter particles on a rotating rough surface: The role of adhesion. Particuology, 53, pp.92-99.

[16] Benabed, A., Boulbair, A., & Limam, K. 2020. Experimental study of the human walking-induced fine and ultrafine particle resuspension in a test chamber. Building and Environment, 171, p.106655.

[17] Habchi, C., Ghali, K., & Ghaddar, N. 2016. Coupling CFD and analytical modeling for investigation of monolayer particle resuspension by transient flows. Building and Environment, 105, pp.1-12.

[18] Kazzaz, M., Habchi, C., Ghali, K., Ghaddar, N., Alotaibi, S., & Chakroun, W. 2017. Micro-particle indoor resuspension under periodic airflows: a numerical-analytical study and experimentations. Building and Environment, 123, pp.299-314.

[19] Al Assaad, D., Yang, S., & Licina, D. 2021. Particle release and transport from human skin and clothing: A CFD modeling methodology. Indoor air, 31(5), pp.1377-1390.

[20] Ren, J., Tang, M., & Novoselac, A. 2022. Experimental study to quantify airborne particle

deposition onto and resuspension from clothing using a fluorescent-tracking method. Building and environment, 209, p.108580.

[21] Whyte, W. 2010. Cleanroom technology: fundamentals of design, testing and operation. John Wiley & Sons.

[22] Zhang, Z., & Chen, Q. 2007. Comparison of the Eulerian and Lagrangian methods for predicting particle transport in enclosed spaces. Atmospheric environment, 41(25), pp.5236-5248.

[23] Pourfarzaneh, A., Jafarian, A., & Kharinezhad Arani, H. 2019. Numerical study of particulate turbulent flow to investigate recovery period in cleanrooms. Scientia Iranica, 26(1), pp.331-345.

[24] Khajenoori, M., & Haghighi Asl, A. 2018. Two-dimensional Simulation of Mass Transfer and Nano-Particle Deposition of Cigarette Smoke in a Human Airway. Journal of Heat and Mass Transfer Research, 5(1), pp.79-85.

[25] Ounis, H., Ahmadi, G., & McLaughlin, J. B. 1991. Dispersion and deposition of Brownian particles from point sources in a simulated turbulent channel flow. Journal of Colloid and Interface Science, 147(1), pp.233-250.

[26] Kao, H. M., Chang, T. J., Hsieh, Y. F., Wang, C. H., & Hsieh, C. I. 2009. Comparison of airflow and particulate matter transport in multi-room buildings for different natural ventilation patterns. Energy and Buildings, 41(9), pp.966-974.

[27] Mahdavimanesh, M., Noghrehabadi, A. R., Behbahaninejad, M., Ahmadi, G., & Dehghanian, M. 2013. Lagrangian particle tracking: model development. Life Science Journal, 10(8s), pp.34-41.

[28] Vahedi, S. M., Parvaz, F., Rafee, R., & Khandan Bakavoli, M. 2018. Computational fluid dynamics simulation of the flow patterns and performance of conventional and dual-cone gas-particle cyclones. Journal of Heat and Mass Transfer Research, 5(1), pp.27-38.

[29] Zhang, P., Roberts, R. M., & Bénard, A. 2012. Computational guidelines and an empirical model for particle deposition in curved pipes using an Eulerian-Lagrangian approach. Journal of Aerosol Science, 53, pp.1-20.

[30] Kraichnan, R. H. 1970. Diffusion by a random velocity field. The physics of fluids, 13(1), pp.22-31.

[31] Sajjadi, H., Salmanzadeh, M., Ahmadi, G., & Jafari, S. 2016. Simulations of indoor airflow and particle dispersion and deposition by the lattice Boltzmann method using LES and RANS approaches. Building and Environment, 102, pp.1-12.

[32] Berlemont, A., Desjonqueres, P., & Gouesbet, G. 1990. Particle Lagrangian simulation in turbulent flows. International Journal of Multiphase Flow, 16(1), pp.19-34.

[33] Zhang, X., Ahmadi, G., Qian, J., & Ferro, A. 2008. Particle detachment, resuspension and transport due to human walking in indoor environments. Journal of Adhesion Science and Technology, 22(5-6), pp.591-621.

[34] Pozorski, J., & Minier, J. P. 1998. On the Lagrangian turbulent dispersion models based on the Langevin equation. International Journal of Multiphase Flow, 24(6), pp.913-945.

[35] Johnson, K. L., Kendall, K., & Roberts, A. 1971. Surface energy and the contact of elastic solids. Proceedings of the royal society of London. A. mathematical and physical sciences, 324(1558), pp.301-313.

[36] Soltani, M., & Ahmadi, G. 1994. On particle adhesion and removal mechanisms in turbulent flows. Journal of Adhesion Science and Technology, 8(7), pp.763-785.

[37] Qian, J. 2007. Particle resuspension via human activity. Ph. D. Thesis.